Immobilization of Cs/Sr fraction of radioactive wastes into phosphorus containing compounds of NZP structure types

Bachelor Thesis

P. R. Jagai

Immobilization of Cs/Sr fraction of radioactive wastes into phosphorus containing compounds of NZP structure types

Priya Jagai
4159101
p.r.jagai@student.tudelft.nl
BSc. Molecular Science and Technology 2013-2014
01-07-2014

Supervisors:
Denis Bykov
Rudy Konings
Jan-Leen Kloosterman

Delft University of Technology
Faculty of Applied Sciences
Department of Radiation Science and Technology
Section of Nuclear Energy and Radiation Applications

Table of Contents

1. Introduction

1.1 Problem of High Level Waste disposal

Nuclear spent fuel can be disposed directly (open fuel cycle) or it can be reprocessed to extract the uranium and plutonium to reduce the total volume of the waste (closed fuel cycle) *(IAEA, 2008)*. A typical 1 GW(e) nuclear power station generates about 1 ton of fission products and minor actinides as high level waste per year *(IAEA, 2012)*. This high level waste (HLW) contains more than 95% of the total radioactivity produced during the nuclear power generation. The majority of radio-toxicity in HLW is caused by minor actinides, which have a relatively longer half-life and increase the total storage time of the waste.

One of the approaches to manage HLW is to separate the waste into several groups to optimize final disposal *(IAEA, 2008)*. Studies suggest to separate the minor actinides for transmutation to reduce their radio-toxicity and required storage time *(Warin, 2011)*.
The total loading of the waste packages of HLW that has to be disposed of underground is temperature limited by the repository requirements (<100 °C) *(Verhoef et al., 2011)*. By removing the heat generating fission products, the volume of the total waste will be significantly reduced *(Law et al., 2006)*. This means that more loading in HLW can be possible before reaching 100 °C in the waste package.

1.2 Fission products: Cesium and strontium

Radioactive isotopes Cs-137 and Sr-90 are the two most heat generating fission products present in HLW. Cs-137 and Sr-90 have a specific power of 0.097 $W.g^{-1}$ and 0.142 $W.g^{-1}$ respectively. Cs-137 has a half live of 30 years and Sr-90 a half-life of 28.8 years. Both emit beta radiation in their decay processes. Cesium and strontium also mimic the chemical properties of respectively potassium and calcium, which are crucial for all organisms. When ingested, they can potentially cause cancer and damage tissue. This may happen when these radionuclides are uptaken by organisms in the food chain trough soil and groundwater. In *(Sims et al., 2008)* the mobility of uranium, cesium and strontium has been studied for prairie soil, collected at the site of 1951 leak from an aqueous solution of irradiated uranium. In this study diffusion coefficients between 0.6 10^{-4} and 3.0 10^{-4} $cm^2.s^{-1}$ for Cs-137 and 1.6 10^{-9} and 2.6 10^{-9} $cm^2.s^{-1}$ for Sr-90 were measured, while the diffusion coefficient for U-238 was between 3.0 10^{-10} and 1.8 10^{-9} $cm^2.s^{-1}$. Cs-137 is the most mobile isotope and U-238 the least among these three isotopes.

Cesium and strontium can be immobilized simultaneously as a single waste form that can to be stored above ground. This requires co-extraction of cesium and strontium.

Simultaneous extraction reduces the total space, facilities, as well as chemical reagents *(Xu et al., 2012; Todd T.A., 2004)*. Several schemes have been developed and demonstrated to separate Cs and Sr simultaneously from dissolved spent fuel. These processes are proven to be extremely efficient *(Law et al., 2006; Xu et al., 2012; Todd T.A., 2004;Todd T.A., 2005)*.
The product stream in tested co-extraction processes consists of 59.2 mole% of cesium and 40.8 mole% of strontium *(Law et al., 2006)*.

1.3 Isolation and solidification of Cs/Sr fraction in phosphate waste forms

The safe isolation of the separated Cs/Sr fraction from the biosphere requires immobilization of the radionuclides in a solid matrix for they have to be disposed for at least three hundred years to decay to a stable isotope. The waste form should possess a chemical, physical, thermal and radiation stability and resist leaching, powdering, cracking, and other modes of degradation and have a good heat conduction. The waste matrix should also be relatively inexpensive for fabrication and easy to handle.

The current technology for disposing HLW is mainly solidification of the entire HLW content in a glass matrix. The disadvantages of vitrification are thermodynamic instability and devitrification *(Mingfen et al., 2012; Montel, 2011)*. In France and UK borosilicate glass is used. Its softening temperature is around 800 °C. In Russia phosphate glass is applied, which has a softening point of approximately 400 °C.

In general, ceramic materials based on the structure of natural minerals draw attention as an alternative to glass, because they excel glass with respect to chemical, thermal and radiation stability *(Clarke, 1983; Montel, 2011; Mingfen et al., 2012;* Orlova, 2002*)*. Ceramic waste forms know classes of oxide and salt ceramics. Some of them belong to the structure types of phosphates. Phosphates are of great interest to act as a host for radioactive waste, such as structure types of natural minerals of monazite, kosnarite, pollucite and many others. Phosphate compounds that may serve as waste forms are inorganic, anhydrous and a selection between orthophosphates and polyphosphates.

Generally phosphates are relatively easy to synthesize. Besides, a phosphorus source may be available in the HLW originating from tri-butyl phosphate (TBP) from the PUREX

process. TBP, however, may be degraded to the more hazard mono- and di-butyl phosphates and recycling options for TBP are also open.

1.4 NASICON phosphates

(Anantharamulu et al, 2011)

Among the phosphate materials, sodium zirconium orthophosphate is $Na[Zr_2(PO_4)_3]$ (NZP) is being studied. The structural analogue of NZP is the natural mineral kosnarite $KZr_2(PO_4)_3$ with space group $R\bar{3}c$ *(Brownfield et al, 1993)*.

Nasicons (Sodium super ionic conductors) are a class of solid electrolytes with structure types $Na_{1+x}Zr_2P_{3-x}Si_xO_{12}$ for $0 \leq x \leq 3$. It is a solid solution of $NaZr_2(PO_4)_3$ (NZP) and $Na_4Zr_2Si_3O_{12}$ (NZS). These compounds have a high ionic conductivity which is used to make devices such as fuel cells and membranes. These structure types also possess of a low thermal expansion and the ability to accommodate ions in the lattice, which makes them interesting as a host for radioactive waste. The special attraction of the Nasicon lies in its structure.

Moreover, zirconium can be present in HLW originating from the zirconium alloy cladding. The presence of zirconium and phosphorous makes it ideal to focus on a framework structure fragment of $[Zr_2(PO_4)_3]^-$ for a "waste into waste" prospect.

1.4.1 Structure of NZP structural type

The chemical formula of sodium zirconium orthophosphate is $Na[Zr_2(PO_4)_3]$ (NZP). The structure of NZP was determined for the first time in 1968 by Hagman et al. NZP crystallizes in a trigonal crystal system, with space group $R\bar{3}c$, with rhombohedral ($a = b \neq c$, $\alpha = \beta = 90^o$, $\gamma = 120^o$) cell parameters of a = 8.8 Å, c = 22.76 Å, Z = 6 *(Hagman et al, 1986)*.

NZP has a framework structure fragment of $[Zr_2(PO_4)_3]^-$ which belongs to the class of anhydrous compounds with oxy-anions described by the general formula $A^IB^{II}R^{III}M^{IV}C^V(XO_4)_n$, where XO_4 is a tetrahedral anion (with X = Si, P, S and Mo) and A^{1+}, B^{2+}, R^{3+}, M^{4+}, and C^{5+} are cations of different oxidation states in the void and framework to compensate the framework charge *n (Orlova, 2002)*.

The crystal chemical formula for the rhombohedral phosphates is $(M1)(M2)_3[L_2(PO_4)_3]$, where M1 and M2 are the void cations and L is the framework cation. The crystal chemical formula for the phosphate $NaZr_2(PO_4)_3$ is $Na\square_3[Zr_2(PO_4)_3]$. The M1 position is occupied by Na, forming a bond with 6 oxygens; the three M2 positions remain vacant

(□) and two L positions are occupied by two Zr, forming ZrO_6 octahedra. Each ZrO_6 octahedra is linked to six PO_4 tetrahedra, and each PO_4 tertrahedra is linked to four ZrO_6 octahedra by sharing the terminal oxygen forming a rigid framework with cavities in between along the c-axis. These cavities can be filled with two types of void cations, M1 and M2. The M1 position lies in between the 2 ZrO_6 octahedra, forming an antiprism sharing 6 oxygens with the framework octahedra. Each M1 position is surrounded by three M2 positions. The M2 position can share 8 oxygen atoms (figure 1) *(Orlova, 2002; Orlova et al., 1996; Gobechiya et al., 2004; Pet'kov et al., 1996)*.

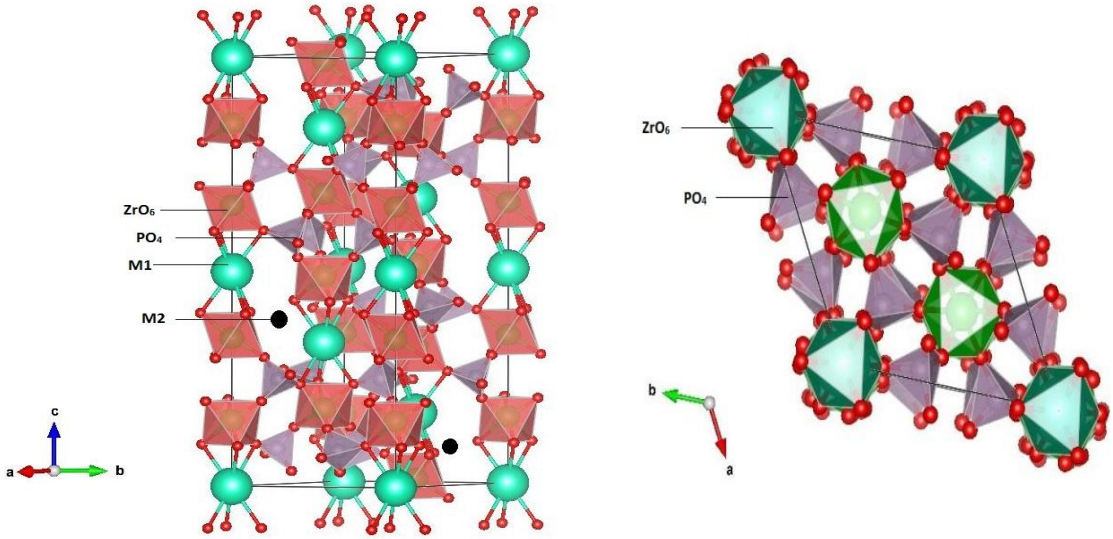

Figure 1 The structure of $Na[Zr_2PO_4)_3]$

1.4.2 Isomorphism in phosphates of the NZP structural type

Isomorphism is the phenomenon of the occurrence of a group of minerals that have the same crystal structure (iso-structural) and in which specific sites can be occupied by two or more elements, ions, or radicals. The term therefore requires the substitution of one or more elements for another element (or elements) in the mineral structure. If the two elements are soluble in a single solid state a "solid solution" is formed.
The Goldschmidt's rule states, if the radii difference between the two cations is less or equal to 15% and the charge difference is less or equal to 2, isomorphism is extensive *(West, 1984)*. The ionic radii difference between Cs and Sr is about 30%. In this study the isomorphic capacity between Cs and Sr is tested.

Many studies have been done on the isomorphism on NZP structural types by exchanging both void and framework cations in $(M1)(M2)_3[L_2(PO_4)_3]$. It may be concluded that the isomorphic capacity in NZP structure types is very big based on experimental studies *(Orlova, 2002)*.

Void and framework cations of oxidation states +1, +2, +3, +4 and +5 are denoted as A, B, R, M and C, respectively and the variety is given below.

M1 = (A) Li, Na, K, Rb, Cs, Cu, Ag
(B) Mg, Ca, Sr, Ba, Mn, Co, Ni, Cu, Zn, Cd
(R) Sc, Fe, Y, Bi, La-Lu
(M) Zr, Hf
M2 = (A) Na, K
L = (A) Na, K
(B) Mg
(R) Al, Sc, Cr, Fe, Ga, Y, In, Eu, Gd, Tb, Dy, Er, Yb
(M) Ti, Ge, Zr, Mo, Sn, Hf, U, Np, Pu
(C) V, Nb, Sb, Ta

According to this data the cationic radii (Å) for different types of positions can be noted: $0.71 \leq r_{(M1)} \leq 1.67$, $1.18 \leq r_{(M2)} \leq 1.51$ and $0.54 \leq r_{(L)} \leq 1.02$.

Generally the cations in the framework that can occupy the L position are smaller than the void cations occupying the M1 position. The M2 position can be occupied by medium sized cations.

In this project Cs and Sr are to be immobilized in NZP structural types with framework $[Zr_2(PO_4)_3]^{-1}$.

To explore the joint insertion of Cs and Sr in NZP structure types, studies of the miscibility is needed.

$CsZr_2(PO_4)_3$ has a space group of $R\bar{3}c$ and a cell volume V of 1599 $Å^3$.
Cs has a relatively big ionic radii of 1.67 Å and can only occupy the M1 position while the M2 position is remained vacant.

Sr (r = 1.18 Å), however is approximately 30% smaller than Cs and can potentially occupy both the M1 and M2 positions according to the isomorphic capacity reviewed in *(Orlova, 2002)*. Compounds as $Sr_{0.5}Zr_2(PO_4)_3$, $Sr_{0.5}Ti_2(PO_4)_3$, $SrFeZr(PO_4)_3$, $SrSmZr(PO_4)_3$ and $Sr_{1.2}Sm_2(PO_4)_3$ have been reported to have the NZP structure type.
$Sr_{0.5}Zr_2(PO_4)_3$ with space group $R\bar{3}$ *(Pet'kov et al., 2002)* and $SrFeZr(PO_4)_3$ with a space group $R\bar{3}c$ *(Sugantha et al., 1994)* were succesfully obtained as representatives of NZP.

In $SrFeZr(PO_4)_3$ Fe occupies one framework position as a charge compensator. For this compound the magnetic and thermal behaviour were studied in *(Sugantha et al., 1994)*.

In the present study the solid solution in all compositional range between $CsZr_2(PO_4)_3$ and $SrFeZr(PO_4)_3$ with the same structure type and Fe as a charge compensator are investigated with formula $Cs_xSr_{(1-x)}[Zr_{(1+x)}Fe_{(1-x)}(PO_4)_3]$.

1.4.3 Properties of NZP

Because of its wide variety of applications, many NZP compounds have been synthesized and different properties were investigated.
$NaZr_2(PO_4)_3$ has low thermal expansion coefficient of about 10^{-6} $^oC^{-1}$ *(Hazen et al., 1987; Pet'kov et al., 2004)*.
These compounds are interesting for their high loading of radioactive isotopes of Cs and Ba *(Gobechiya et al., 2004)*.

Investigation on the leachability of NZP compounds were carried out. The leaching rate of $CsZr_2(PO_4)_3$ was found to be 0.04 mg m^{-2} day^{-1} in deionised water, 90 ^oC after 7 days *(Naik et al., 2010)*. $SrFeZr(PO_4)_3$ was found to have a leaching rate of 0.22 mg m^{-2} day^{-1} after 16 days of experiment in deionised water, 90 ^oC *(Sugantha et al., 1998)*.

In *(Pet'kov et al., 2013)* the thermodynamic properties of $CsZr_2(PO_4)_3$, such as the molar heat capacity, enthalpy and entropy were investigated.

NZP compounds are proved to be extremely stable compounds. A review in 2004 summarizes all the studies done on thermo physical properties of certain NZP compounds *(Pet'kov et al., 2004)*. Structural analogues of NZP are structurally stable up to very high temperatures for example the decomposition temperatures of $NaZr_2(PO_4)_3$ and $Sr_{0.5}Zr_2(PO_4)_3$ are 1650 ^oC and 1700 ^oC respectively.

Studies such as *(Bykov et al., 2005; Bykov et al., 2006; Barre et al., 2005)* have investigated the behaviour of lanthanides and actinides in the NZP matrix. *(Gregg et al., 2014)* have investigated recently the effect of α-decay simulated by ion beam irradiation of He and Au ions on $SrFeZr(PO_4)_3$.

The aim of this project was to test the inclusion of Cs and Sr simultaneously in the NZP with Fe and Zr in the framework. A series of compounds with general formula $Cs_xSr_{(1-x)}[Zr_{(1+x)}Fe_{(1-x)}(PO_4)_3]$ was synthesized with different methods. Different techniques were

applied for investigation on properties and structure characterization, namely ICP-OES, XRD, Soxhlet leaching test and Mössbauer spectroscopy.

2. *Synthesis*

2.1 Reactants and solutions

For the synthesis of NZP structural type compounds the following chemicals were used: nitrates of cesium, $Cs(NO_3)$ (Alfa Aesar, 99.9%) and strontium, $Sr(NO_3)_2$ (Sigma-Aldrich, >99%), phosphoric acid, H_3PO_4 (1.45 M), diammonium monohydrogen phosphate powder $(NH_4)_2HPO_4$, solution of iron nitrate, $Fe(NO_3)_3$ (0.42 M) and zirconium oxychloride solution $ZrOCl_2$ (0.38 M).

The solutions of iron nitrate and zirconium oxychloride were made of crystal hydrates: $Fe(NO_3)_3.9H_2O$ and $ZrOCl_2.8H_2O$, respectively. The salts were dissolved in water to prepare solutions. The concentrations were determined by Inductively Coupled Plasma Optical Emission Spectrometry (ICP-OES). The ICP analysis used a standard with known concentration to determine the actual concentration of the solutions.

2.2 Experimental synthesis methods

In this work three different procedures were used for the synthesis of Cs and Sr containing compounds with the NZP structure type: namely the sol-gel, mechano-chemical synthesis and hydrothermal synthesis.

2.2.1 Sol-gel

In the sol-gel method the starting materials, which are aqueous solutions of metal nitrates and phosphoric acid, are added in stoichiometric amounts together forming a precipitation. This suspension is mixed to reach homogeneity. The liquid is removed by a drying process. Afterwards the powder undergoes a heat treatment for denitration at 600 ^{o}C for 12 hours. At this temperature the powder is not yet crystallized. Therefore the samples undergo other heat treatments to crystallize at 800 ^{o}C for 24 hours and 1000 ^{o}C for 6 hours. Between the heating steps grinding of the samples was done for homogenization. This was done with a agate mortar and a vibration mill. A schematic representation of the sol-gel procedure is illustrated in figure 2.

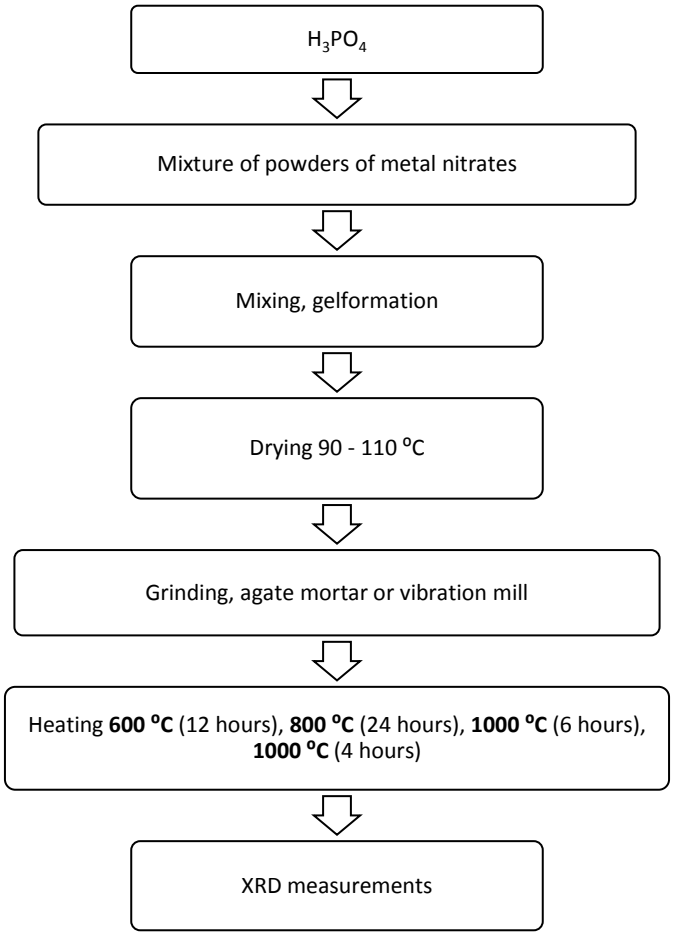

Figure 2 A schematic representation of the sol-gel procedure

2.2.2 Mechano-chemical synthesis

Mechano-chemical synthesis is a dry, high-energy ball milling powder processing technique that allows production of homogeneous materials starting from blended elemental powder mixtures. The planetary ball mill of Retch PM400 was used.

Important parameters are speed and duration of the milling, the ball to powder ratio (BPR) and the materials of the milling jars and balls.

Milling jars and balls made of tungsten carbide were used.

The precursor powder, which is synthesized with the sol-gel method, is mechanically ground at high rotation speed of 400 rpm for 8 hours at room temperature to form an amorphous phase. The ball milling is done with a BPR of 20:1. After the mechanical activation of the compound, it is treated at high temperature of 1000 ˚C for 6 hours for crystallization (figure 3).

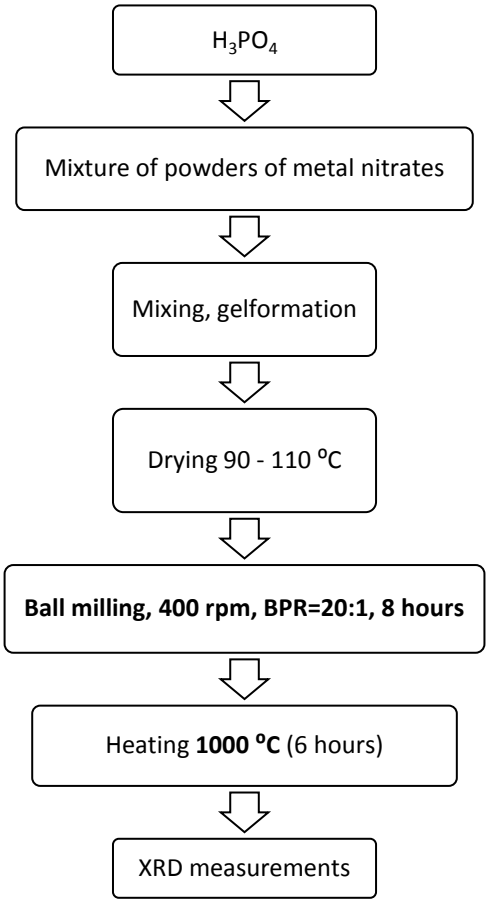

Figure 3 A schematic representation of the ball milling procedure

2.2.3 Hydrothermal synthesis

The term 'hydrothermal' came from the earth sciences, where it implied a regime of high temperatures and water pressures. This method crystallizes a substance directly from the solution depending on the solubility of the substance in super-saturation while cooling it down gradually.

Major differences between hydrothermal processing and other technologies are *(Somiya et al., 2000)*:

1. Powders are formed directly from solution
2. Powders are anhydrous, crystalline or amorphous. It depends on producing of hydrothermal powder temperature
3. It is able to control particle size and shape by hydrothermal temperature
4. It is able to control chemical, composition, stoichiometry
5. Powders are highly reactive in sintering
6. Powders do not need calcination

7. Powders do not need milling process

Hydrothermal synthesis experiments are carried out in typical high temperature, high pressure apparatus called autoclaves. They consist of different compartments, such as, Teflon jars, a safety spring and disks (figure 4).
In this study autoclaves of 23 ml of Parr Instrument Company were used.

Figure 4 Different compartments of typical autoclaves used for hydrothermal synthesis

A total mixture of reactant powders of 200 mg and 9 ml of water were put in the PTFE jars of the autoclave. The mixture was heating until 200 ^{o}C and kept there for three days. Afterwards the mixture was cooled slowly to room temperature. The obtained powder was filtered and washed with deionised water (figure 5).

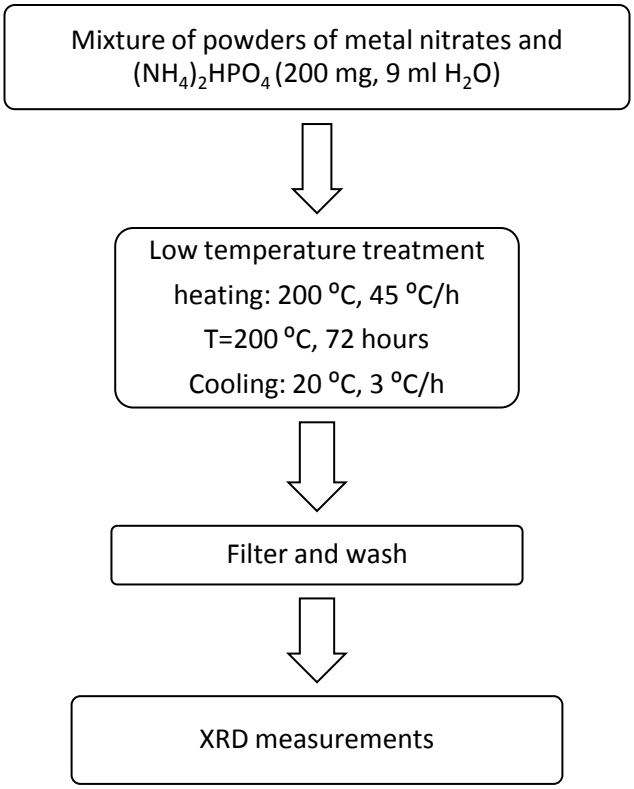

Figure 5 A schematic representation of the hydrothermal synthesis method

3 Characterization and Investigation methods

3.1 X-ray diffraction for characterization

The phase analysis of the compounds was done by X-ray diffraction. The XRD measurements for phase analysis were done at 45 kV, 40 mA in the 2θ range of 10 °- 50 °, λ(CuK_α) = 1.54046 Å with the instrument X'pert Pro MPD DY2977. The phase analysis was done with the software Panalytical X'pert Highscore. The obtained diffractogrammes were compared to standard patterns which are collected in the Powder Diffraction File. The cell parameters were calculated by the programme Fullprof*(Rodriguez-Carvajal, 1993)* and the structures were plotted by Vesta *(Momma, 2013)*.

3.2 Soxhlet leaching test for chemical durability

The idea of immobilizing radioactive waste in ceramic waste forms for long-term disposal, requires among others chemical stability and durability.
The leachability is an important factor for the evaluation of long term chemical durability of solid waste forms. The highest resistance against leaching of the radionuclide in the leachate is desired. In this context, normalized leach rates of lower than $1 g.m^{-2}.day^{-1}$ at temperatures below 100 °C are considered as baseline according to *(Vance, 2012)*.

The Soxhlet extraction technique is widely used to determine the leaching rate of solid waste forms. Each time the sample is in contact with fresh leachate. After a certain time the concentration of the ions leached from the pellet in the leachate can be measured. A leaching test setup is shown in figure 6.

Figure 6 The leaching test set up used in this technique

For the leaching test the medium (leachate) and pellet (sample) preparations are important.
The medium was prepared with 300 ml of deionised water. The temperature of the medium in contact with the pellet was 95 ^{o}C.
For sample preparation the powder was pressed at 100 MPa to a pellet and sintered at 1000 ^{o}C for 6 hours. The pellet had a 64% theoretical density and a surface area of 358 mm^2.

The normalized mass loss from the pellet and the leaching rate of species *i* can be calculated with the following formulas:

$NL_i = (C_i \times V) / (f_i \times SA)$ (mg.m^{-2})

$R_i = NL_i/days$ (mg.m^{-2}.d^{-1})

- NL_i = normalized mass loss of species *i*
- R_i = leaching rate
- C_i = Concentration of species *i* (mg/L)
- V = solution volume (L)
- f_i = mass fraction of element *i* in the unleached solid (pellet)
- SA = Surface area specimen (m^2)

In this experiment the leaching rate of Sr in $SrFeZr(PO_4)_3$ was determined. The Sr mass fraction in this compound is 17%.
This experiment was carried out for 27 days. Probes were taken on the 3rd, 10th, 17th and 27th day. The concentration of species *i* from the unleached solid in the leachant was measured by ICP-OES.

3.3 Characterization with Mössbauer spectroscopy

Mössbauer spectroscopy was first observed by Rudolf Mössbauer when he did his PhD work in 1958. He received a Nobel prize for his research concerning the resonance absorption of gamma radiation in 1961.

Mössbauer spectroscopy is concerned with the recoil-free transitions that take place inside the atomic nuclei.
Only a limited number are isotopes are suitable for Mössbauer work for example ^{57}Fe, ^{119}Sn, ^{129}I.
A nucleus emits γ-radiation (^{57}Fe). This radiation is filtered/screened/varied by using the Doppler effect. The incident monochromatic beam of radiation is then absorbed by the sample (Fe) and the out coming beam is monitored as a function of energy.
The energy of the γ-ray from the source is varied by the Doppler effect: the sample is fixed in a certain position and the γ-ray source is moved at a constant velocity either away or towards the sample (+V, -V). In this way different energies of the γ-rays are determined against the different velocities.

The spectrum that is obtained (absorption vs velocity) consists of poorly resolved peaks. An appropriate analysis of this data may give information about the ***local*** structure, oxidation states, coordination numbers and bond character *(West, 1984)*.

Data analyzing can be done by finding hyperfine individual parameters, that characterize a measured spectrum. These parameters can be easily extracted from many software packages and fitted to the experimental spectra. Distribution of electric quadrupole splittings (QS in $mm.s^{-1}$) and isomer shifts (IS in $mm.s^{-1}$) are useful in characterizing the local environment of iron in different phases.

Transmission ^{57}Fe Mössbauer absorption spectra were collected at 300 K with a conventional constant-acceleration spectrometer using a 57Co(Rh) source. Velocity

calibration was carried out using an α-Fe foil. The Mössbauer spectra were fitted using the Mosswinn 4.0 program.

This study was done on (x=0) $SrFeZr(PO_4)_3$ and (x=0.6) $Cs_{0.6}Sr_{0.4}Zr_{1.6}Fe_{0.4}(PO_4)_3$.

4 Results and discussion

In this study the solid solution between $CsZr_2(PO_4)_3$ and $SrFeZr(PO_4)_3$ belonging to the NZP structure type were investigated with formula $Cs_xSr_{(1-x)}[Zr_{(1+x)}Fe_{(1-x)}(PO_4)_3]$ for x = 0, 0.2, 0.4, 0.6, 0.8, 1.

Synthesis with Sol-gel method

A profile fitting was done after the XRD measurements for compounds synthesized at 1000 ° by the **sol-gel** method. The diffractogrammes are given in figure 7 and the results of the phase analysis are given in table 1.

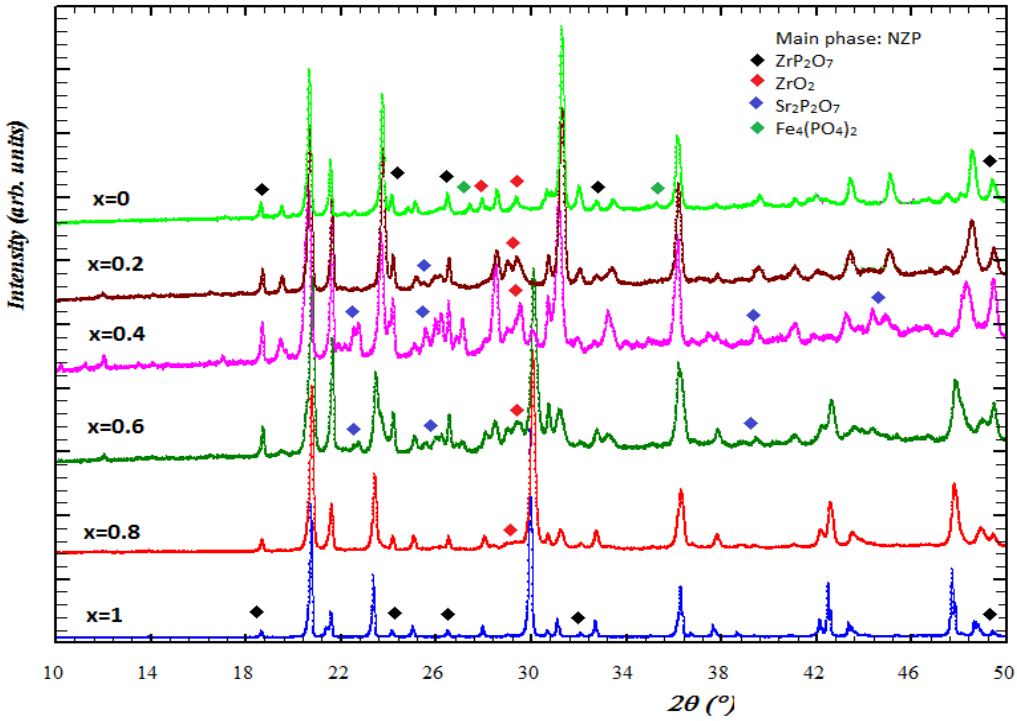

Figure 7 XRD data for $Cs_xSr_{(1-x)}[Zr_{(1+x)}Fe_{(1-x)}(PO_4)_3]$ for x = 0, 0.2, 0.4, 0.6, 0.8, 1 after 1000 °C with sol-gel

Table 1 Phase analysis results for the simultaneous inclusion of Cs and Sr in NZP structural type compounds $Cs_xSr_{(1-x)}[Zr_{(1+x)}Fe_{(1-x)}(PO_4)_3]$

x	Phase analysis
1	$CsZr_2(PO_4)_3$ (NZP) and ZrP_2O_7
0.8	$CsZr_2(PO_4)_3$, (NZP) ZrP_2O_7 and traces of admixtures
0.6	$CsZr_2(PO_4)_3$, (NZP) ZrP_2O_7 and admixtures
0.4	$SrFeZr(PO_4)_3$, (NZP) ZrP_2O_7, $Sr_2P_2O_7$ and other admixtures
0.2	$SrFeZr(PO_4)_3$, (NZP) ZrP_2O_7 and other admixtures
0	$SrFeZr(PO_4)_3$, (NZP) ZrP_2O_7, ZrO_2 and $Fe_4(PO_4)_2$

According to the phase analysis a whole row of NZP solid solution on structure type exists between $CsZr_2(PO_4)_3$ and $SrFeZr(PO_4)_3$. However, a secondary phase of ZrP_2O_7 was formed.

The diffractograms for these two end members were different, although they have the same structure type.

Profile fittings have been done with Fullprof for all the compounds. These results indicate that NZP was the major phase.

For x = 1 the phases ZrP_2O_7 and $CsZr_2(PO_4)_3$ (NZP) were formed. This means there should be an excess of Cs in the powder forming other phases. The diffractogram shows no traces of other crystalline Cs compounds. This could be because Cs evaporated as it is known that Cs is a volatile element or formed an amorphous phase.

A two-phase profile fitting with Fullprof shows a good fit of both phases with no residual peaks (no admixtures) with a R_{wp} of 24% in figure 8.

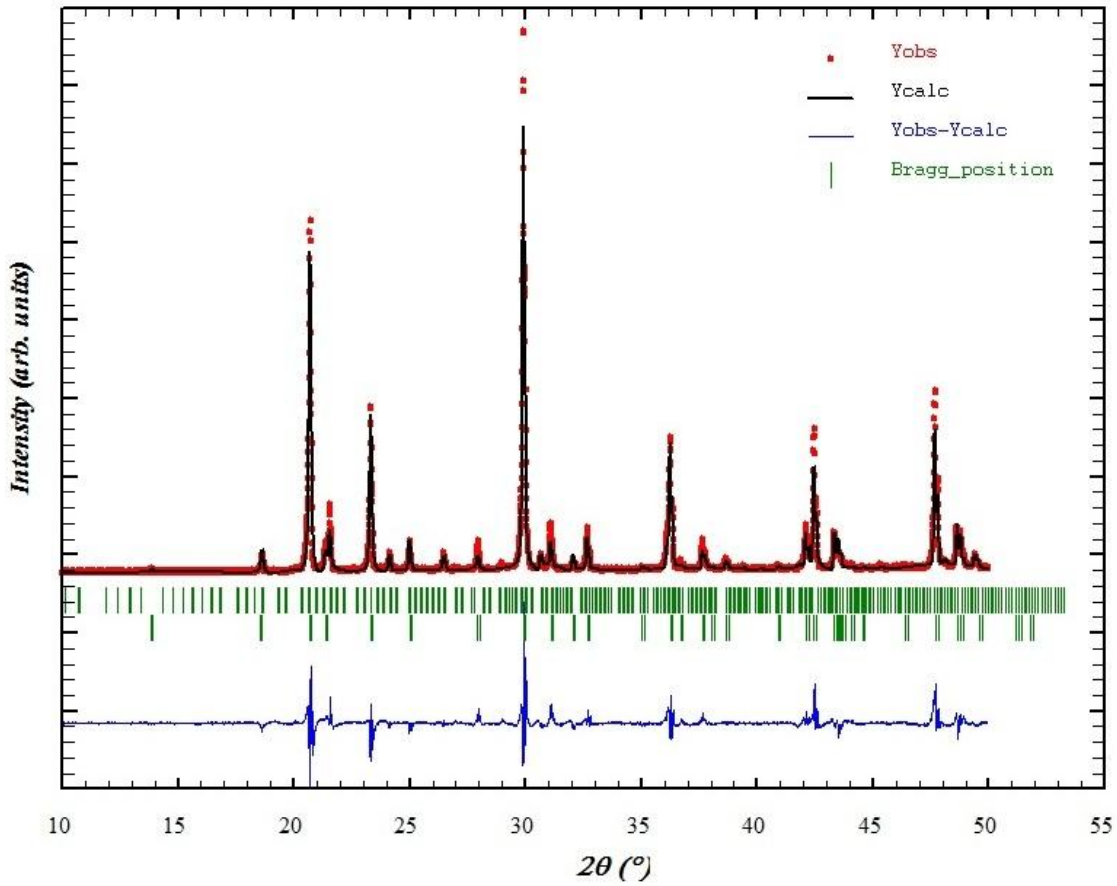

Figure 8 A two-phase profile fitting for x=1 with sol-gel: ZrP_2O_7 and $CsZr_2(PO_4)_3$

For x = 0 the major phases were $SrFeZr(PO_4)_3$ (NZP) and ZrP_2O_7 as indicated in table 1. Other admixtures were formed, such as ZrO_2 and $Fe_4(PO_4)_2$.

Synthesis by mechano-chemical method

The results for the solid solution $Cs_xSr_{(1-x)}[Zr_{(1+x)}Fe_{(1-x)}(PO_4)_3]$ with **ball milling** after 1000 ^oC for x = 0, 0.2, 0.4, 0.5, 0.6, 0.8, 1 are given below in figure 9.

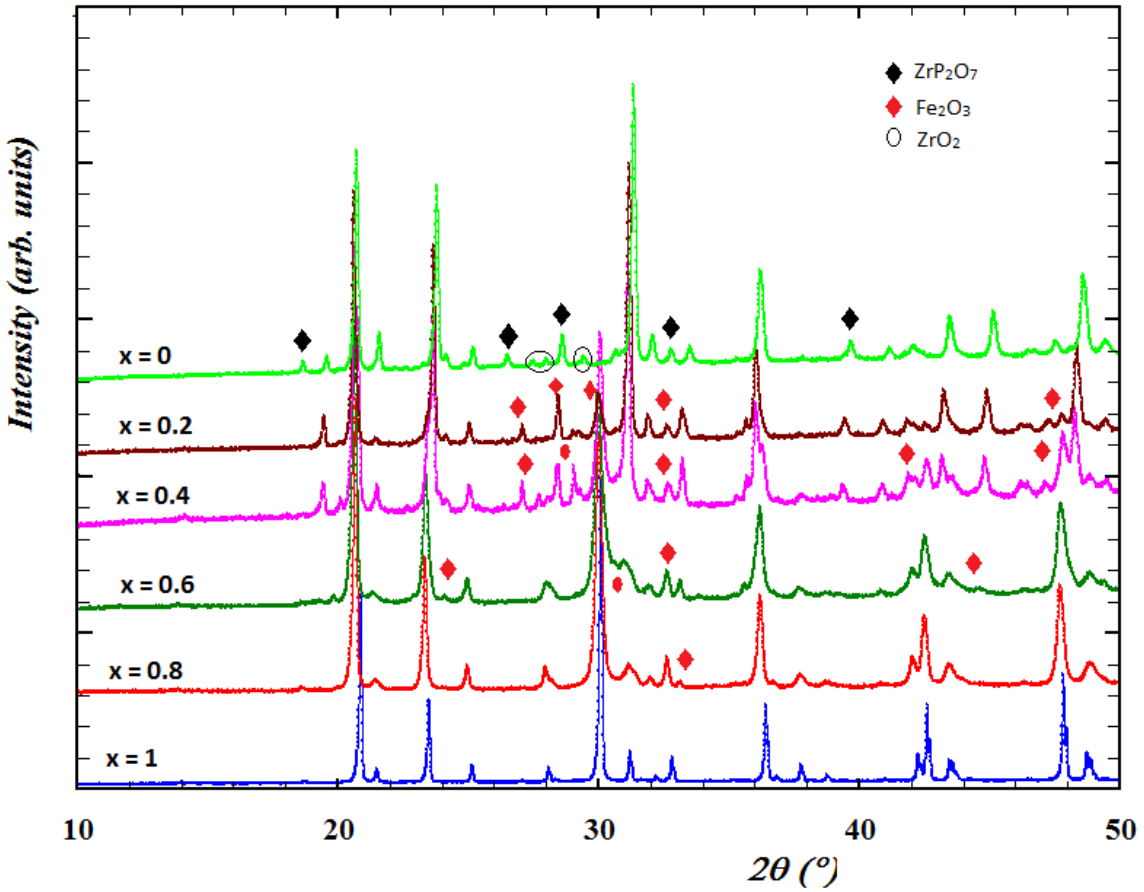

Figure 9 XRD data for $Cs_xSr_{(1-x)}[Zr_{(1+x)}Fe_{(1-x)}(PO_4)_3]$ for x = 0, 0.2, 0.4, 0.6, 0.8, 1 after 1000 °C with ball milling

By this method a whole row of solid solution was obtained with considerably less amount of admixtures compared to the sol-gel method. The impurities are ZrP_2O_7, Fe_2O_3 and ZrO_2.

For x = 1 a pure phase of $CsZr_2(PO_4)_3$ was obtained.

For x = 0 the major phases were $SrFeZr(PO_4)_3$ (NZP) and ZrP_2O_7. In smaller amounts, ZrO_2 was detected. After profile fitting the phase weight composition was analyzed. This compound consisted of 85% of NZP phase. There is a possibility that Zr and P were in excess. Or the contact between all the atoms was somehow not enough stimulated by ball milling to form a single phase. Another possibility is that the compound starts to decompose at this temperature.

The intermediate compounds of the solid solution were also good quality NZP structural analogues. However Fe_2O_3 was also detected. This may have happened because an excess of Fe during synthesis.

Another explanation may be that the compositional range of inclusion of Fe in the structure is less than 1. This behaviour is due to the radii difference of 10.4% between the smaller Fe^{3+} and bigger Zr^{4+} cation. This observation was also made in *(Miyajima et al., 1996)*, where Zr was substituted by lanthanides (Ln) with oxidation states of +3. The bigger the radii of the Ln cations, the smaller the solubility limit in the solid solution.
To explore the occupancy of Fe in $Cs_xSr_{(1-x)}[Zr_{(1+x)}Fe_{(1-x)}(PO_4)_3]$, the solubility between $SrFeZr(PO_4)_3$ and $Sr_{0.5}Zr_2(PO_4)_3$ should be tested. There is a possibility that there is a certain optimum for the occupancy of Fe as illustrated in figure 10.

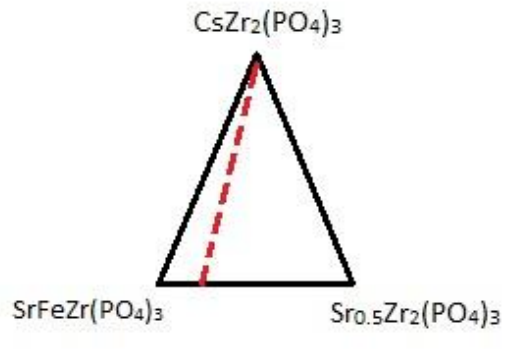

Figure 10 a schematic diagram for the NZP stability range

Hydrothermal synthesis

With the **hydrothermal synthesis** $CsZr_2(PO_4)_3$ (x=1) and x=0 were prepared.

For $CsZr_2(PO_4)_3$, the reactant powders were directly inserted in the PTFE jars of the autoclaves, without any pre-treatments.

The obtained powder was zirconium dioxide ZrO_2.Under these hydrothermal conditions cesium and phosphorus did not react, while $ZrOCl_2$ decomposed to ZrO_2.

For x=0, a precursor powder, which was synthesized with sol-gel and activated mechanically with ball mill, was inserted in the PTFE jars of the autoclaves.

After the hydrothermal synthesis the powder was washed and ground. XRD phase analysis showed that the powder consists of iron phosphate $FePO_4$ and an amorphous phase containing Sr, Zr and P.
The powder was heat treated at 1000 ^oC for 6 hours. A phase analysis showed the formation of NZP phase $Sr_{0.5}Zr_2(PO_4)_3$, ZrP_2O_7 and $FePO_4$ which was already formed before the heat treatment.

Iron phosphate was formed during hydrothermal synthesis and after 1000 ^{o}C it became more crystalline. This caused a lack of Fe and may be the reason of the formation of $Sr_{0.5}Zr_2(PO_4)_3$ instead of $SrFeZr(PO_4)_3$. The remaining Zr formed the pyrophosphate phase.

The parameters for the hydrothermal synthesis can be optimized. This requires more experimental work.

Comparison of synthesis methods

A comparison of all the synthesis methods used in this study to prepare $Cs_xSr_{(1-x)}[Zr_{(1+x)}Fe_{(1-x)}(PO_4)_3]$ for x = 0 - 1 is reviewed. The phase analysis results are given in table2.

Table 2 A comparison of methods Sol-gel, ball milling and hydrothermal synthesis for $Cs_xSr_{(1-x)}[Zr_{(1+x)}Fe_{(1-x)}(PO_4)_3]$

x	***Sol-gel***	***Mechano-chemical Synthesis***	***Hydrothermal synthesis***
0	NZP, ZrP_2O_7, Fe_2O_3, ZrO_2	NZP, ZrP_2O_7, ZrO_2	$Sr_{0.5}Zr_2(PO_4)_3$, ZrP_2O_7, $FePO_4$
0.2 - 0.8	NZP, ZrP_2O_7, Fe_2O_3, ZrO_2	NZP, Fe_2O_3	n.a.
1	NZP, ZrP_2O_7	NZP	No reaction

From table 2 it can easily be concluded that with the ball milling the least of admixtures were obtained. The diffractograms indicated that a good quality of crystalline compounds were formed. Therefore, for further investigation of properties we selected compounds prepared by ball milling.

NZP phase formation in the system

Unit cell parameters for the NZP phase of the whole row of $Cs_xSr_{(1-x)}[Zr_{(1+x)}Fe_{(1-x)}(PO_4)_3]$ synthesized with sol-gel were calculated with Fullprof after profile fittings. The unit cell parameters and volume behaviour when Cs is gradually substituted by Sr is given in the graph below (figure 11).

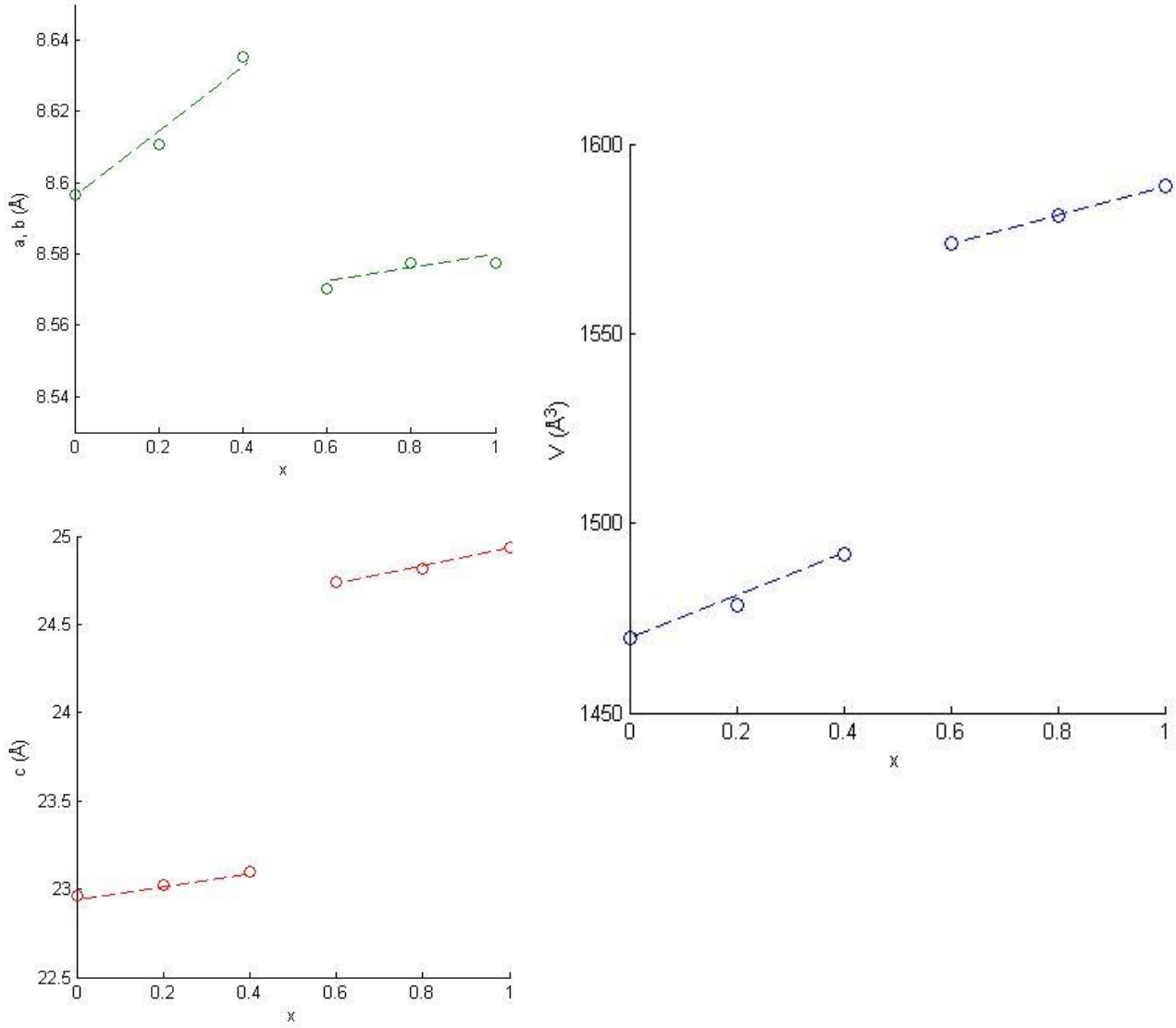

Figure 11 The unit cell behavior of NZP as a function of Cs and Sr content in $Cs_xSr_{(1-x)}[Zr_{(1+x)}Fe_{(1-x)}(PO_4)_3]$

Sr has a smaller ionic radius than Cs. The size of the Sr cation leads to decrease of the cell volume. This leads to a contraction along the c-axis, while the cell parameter along the a-axis does not significantly change. This behaviour proves that Sr has indeed been inserted in the NZP structure matrix. Å

Structure type NZP phase was formed as a major phase and the cell parameters were decreasing with decreasing ionic radii, which means that the intermediate compounds between CsNZP and SrNZP also have the same structure type. Because of ZrP_2O_7 there is an excess of Sr and Cs in the powder. Cs can/may have easily evaporated at 1000 ^oC, but Sr forms another phases of $Sr_2P_2O_7$.

It should be noted that between x=0.4 to 0.6 there is a certain deviation in cell behaviour. According to the cell parameters behaviour, the crystal structures CsNZP and SrNZP are different. For $0 \leq x \leq 0.4$ the NZP phase tends to take the crystal structure of $SrFeZr(PO_4)_3$, as indicated in table 1. On the other hand for $0.6 \leq x \leq 1$ NZP, the NZP phase of $CsZr_2(PO_4)_3$ was analyzed. As mentioned earlier, $CsZr_2(PO_4)_3$ and $SrFeZr(PO_4)_3$ have different XRD patterns. But according to literature (Sugantha et al., 1994) these two compounds have the same space group, namely $R\bar{3}c$. The the dependence of unit cell parameters obtained in this study might indicate that there may be a change in space group depending in the Sr and Cs content. In order to prove this detailed structure investigations by the Rietveld method are needed.

A two-phase Rietveld refinement was done on x=0 (figure 12). The phases $SrFeZr(PO_4)_3$ and ZrP_2O_7 were refined.

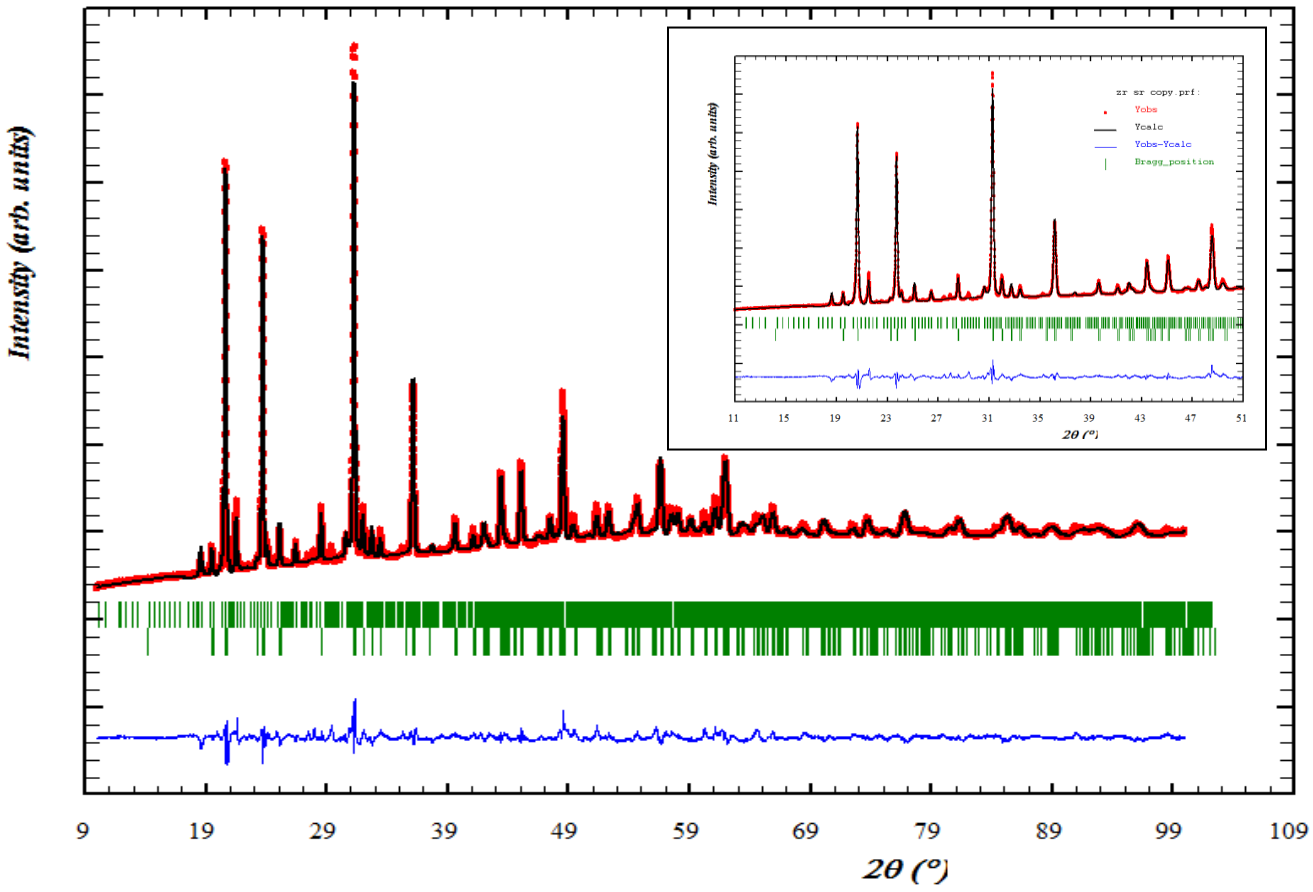

Figure 12 A Rietveld refinement for x = 0, $Cs_xSr_{(1-x)}[Zr_{(1+x)}Fe_{(1-x)}(PO_4)_3]$

The refinement shows a moderate fit of both phases with a R_{wp} of 15%. The space group model for $SrFeZr(PO_4)_3$ was R-3c. However, a perfect fit of less than 5% could not be

reached, even though all the parameters were refined. This could also indicate a change in space group.

Leaching tests on $SrFeZr(PO_4)_3$

The leaching test was carried out for 27 days. Probes were taken out 4 times. The concentration Sr^{2+} in the leachate was determined with ICP-OES. The normalized mass loss and leaching rate was calculated with the formula described in chapter 3.1 and plotted in the graphs below (figure 13).

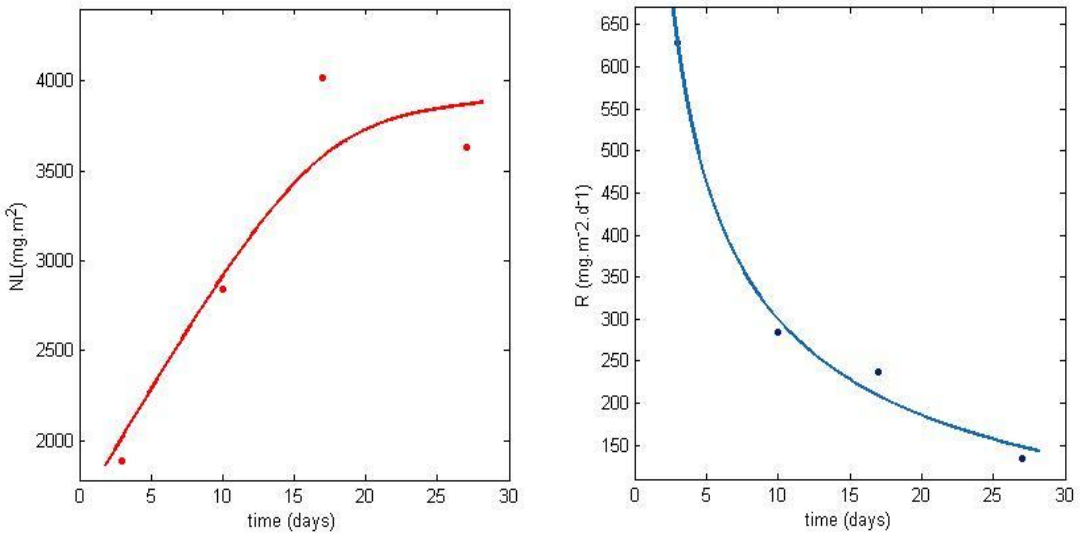

Figure 13 The normalized mass loss (NL) and leaching rate (R) of Sr^{2+} from $SrFeZr(PO_4)_3$

According to the results in figure 10 the normalized mass loss increases over time. The total amount of leached Sr from the pellet is accumulated over time. The leach rates of solids tend to decrease with increasing leaching time even at high degrees of dilution. This is generally attributed to the presence of 'active surface sites' on the cut or polished prepared surface of a candidate solid.

The leaching rate of Sr from $SrFeZr(PO_4)_3$ on the 17^{th} day is 236 mg m^{-2} day^{-1}. $SrFeZr(PO_4)_3$ was found to have a leaching rate of 0.22 mg m^{-2} day^{-1} after 16 days of experiment in deionised water, 90 ^{o}C in the work of *(Sugantha et al., 1998)*. In this work a surface area of 2 m^2/g of the powder was determined.

The minimal leaching rate was determined graphically from the mass loss as a function of time. This was found to be 17 mg m^{-2} day^{-1}. This value is below the baseline of 1 g m^{-2} day^{-1} for waste forms to reach desirable performance, for example synroc.

When assumed that the same mass of the powder was used, the normalized mass loss can be calculated. In the work of Sugantha et al. the normalized mass is 0.53 $mg.d^{-1}$ for the powder. It is assumed that this powder has 100% porosity, which means the maximum leach rate.
In this work the normalized mass loss for the minimal leach rate is 0.0067 $mg.d^{-1}$ of the pellet. This value is obtained with 64% of theoretical density of the pellet. It is further assumed that the powder density, which is not calculated, is within 5% value range of the theoretical density. This means that a porosity of 36±5 % can be obtained.

These calculations indicate that the mass loss for the pellet with a relatively high porosity is lower than the mass loss of the powder obtained in Sugantha et al.

The pellet was relatively not very dense and therefore very porous. This means that the actual surface area of the pellet is much bigger than the calculated value of the pellet. This would give a much smaller leaching rate.

The pellet of $SrFeZr(PO_4)_3$ was measured by XRD after the leaching. The data is shown in figure 14.

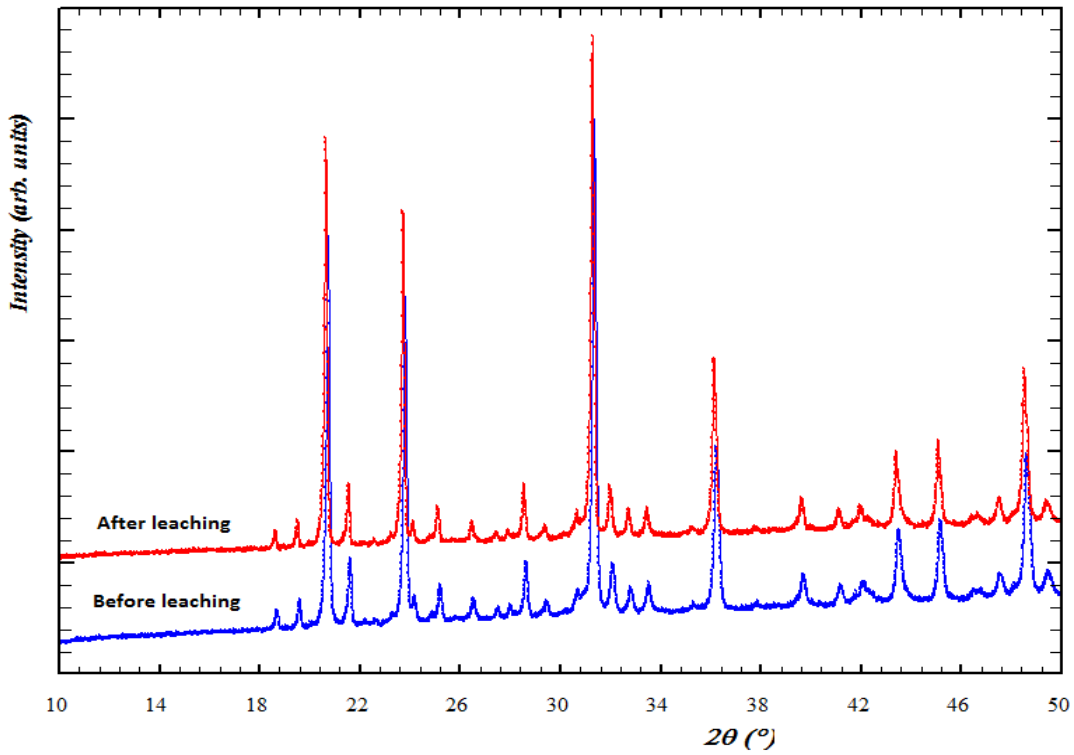

Figuur 14 XRD data for $SrFeZr(PO_4)_3$ before and after the leaching test

The diffractogrammes show no changes, which means no phase alterations after leaching. The NZP structure and the crystallinity are still intact after a certain amount of leached Sr.

Characterization with Mössbauer spectroscopy

The compounds $Sr[FeZr(PO_4)_3)]$ (x=0) and of $Cs_{0.6}Sr_{0.4}[Zr_{1.6}Fe_{0.4}(PO_4)_3]$ (x=0.6) have been characterized with Mössbauer spectroscopy. In table 3 the parameter isomer shift (IS), quadrupole splitting (QS) and spectral contribution of iron in their corresponding phases are given. The Mössbauer spectra for x=0 and x=0.6 were obtained at 300 K and is plotted in figure 15.

Tabel 3 The Mössbauer fitted parameters for x = 0 and x = 0.6 of $Cs_xSr_{(1-x)}[Zr_{(1+x)}Fe_{(1-x)}(PO_4)_3]$

Sample	IS ($mm.s^{-1}$)	QS ($mm.s^{-1}$)	Phase	Spectral contribution (%)
x = 0	0.46	0.21	Fe^{3+}	100
x = 0.6	0.48	0.35	Fe^{3+}	36
	0.38	-0.22	Fe^{3+} (α-Fe_2O_3)	64

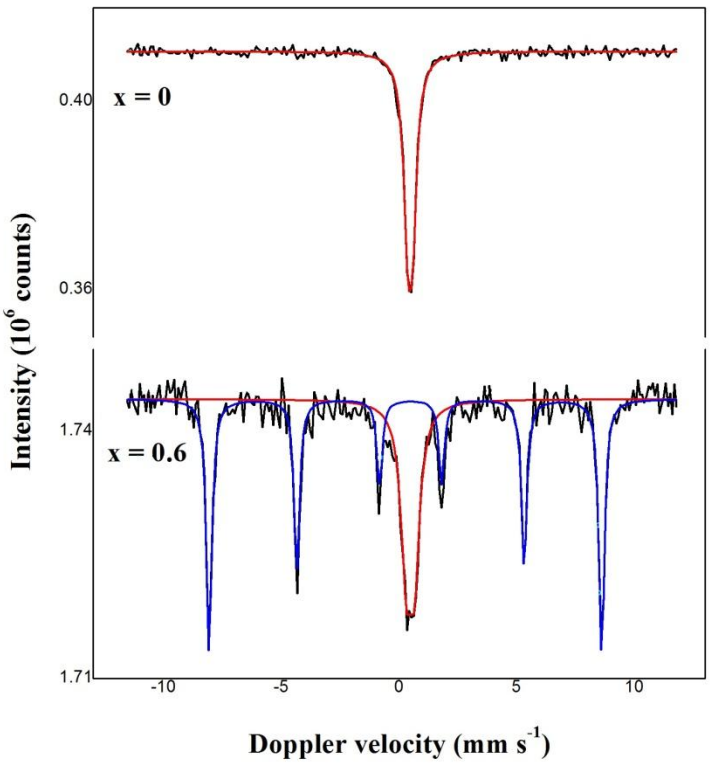

Figure 15 Mössbauer spectra obtained at 300 K for x = 0 and x = 0.6 of $Cs_xSr_{(1-x)}[Zr_{(1+x)}Fe_{(1-x)}(PO_4)_3]$

The spectrum of $Sr[FeZr(PO_4)_3)]$ (x=0) was fitted with a single contribution from high-spin Fe^{3+} cations in octahedral environment (figure 11).
The obtained Mössbauer parameters in table 3: isomer shift, IS = 0.46 mm/s and quadrupole splitting, QS = 0.21 mm/s are in good agreement with previous data on Fe phosphates *(Asabina et al., 2006)*.
The QS value is a direct measure of the degree of distortion of the FeO6 octahedra.
The QS = 0.21 mm/s value is quite small, as compared with the values reported for other Fe phosphates, indicating improved symmetry of the FeO6 octahedra in compound x=0.

The Mössbauer spectrum obtained for x=0.6 reveals the presence of only 36% Fe^{3+} cations in a phosphate configuration. The QS value increased to 0.35 mm/s; probably due to the presence of the additional Cs atoms, distorting the FeO6 octahedra.
The main spectral contribution, 64% in x=0.6, was unambiguously assigned to hematite (α-Fe_2O_3) structures. The reddish color in x = 0.6 is most likely related to the presence of hematite.

Overall, the interaction of the Fe atoms with the surrounding lattice is very small for x=0.6, as a very low signal-to-noise ratio was obtained after five days of measurement. The Mössbauer spectrum of x = 0 was obtained in one day.

For x = 0.6 recalculations of the spectral contribution of iron to the contribution of NZP phase and hematite phase were 91% and 9% respectively. These results are in good agreement with the results obtained with profile fitting of the diffractogramme, which were 93% of NZP phase and 7% of hematite.

Conclusion

In this work the inclusion of Cs/Sr fraction in phosphorus based compounds with the NZP structure types with general formula $Cs_xSr_{(1-x)}[Zr_{(1+x)}Fe_{(1-x)}(PO_4)_3]$were tested with different methods. According to XRD phase analysis it can be concluded that with mechano-chemical synthesis the least of admixtures were obtained. The cell parameter behaviour as a function of compositions x = 0, 0.2, 0.4, 0.6, 0.8, 1 may suggest that the crystal structures of $CsZr_2(PO_4)_3$ and $SrFeZr(PO_4)_3$ are different. For $0 \leq x \leq 0.4$ the NZP phase tends to take the symmetry of $SrFeZr(PO_4)_3$, while for $0.6 \leq x \leq 1$, the $CsZr_2(PO_4)_3$ symmetry was formed. Nevertheless, the structure type for all the compositions were NZP.

The leaching tests on $SrFeZr(PO_4)_3$ indicated a minimal leaching rate of 17 mg m^{-2} day^{-1}, which is below the baseline of a good waste form. After leaching the NZP phase did not alter.

Characterization with Mösbauer spectroscopy confirmed the formation of hematite and NZP in x = 0.6. The mass phase percentages found with this technique were for NZP and hematite 91% and 9% respectively. These results agreed with the weight percentages of both phases obtained with XRD.

Future work

In the future investigations of the thermal properties on NZP compounds should be carried out with DTA/TG in order to determine the decomposition temperatures. Irradiation effects on the structural and macroscopic properties will be tested to establish their performance after exposure to high dose rates.. Also the crystal structure of $SrFeZr(PO_4)_3$ should be solved and the unit cell behaviour should be understood more clearly.

The mechano-chemical synthesis can be used to synthesize other other structure types for example polluicites. The properties of these compounds will be investigated and compared to the NZP structure types.

References

A.I. Shchelokov, Petkov V.I., Egorkova O.V.; 1996; On the existence of phases with a structure of $NaZr_2(PO_4)_3$ in series of binary orthophosphates with different alkaline element to zirconium ratios; J. Struct. Chem. 37, no. 6; 933-940.

Anantharamulu N., Koteswara Rao K., Rambabu G., Vijaya Kumar B., Velchuri R., Vithal M.; 2011; A wide-ranging review on Nasicon type materials; J. Mater. Sci. 46; 2821-2837.

Barre M., Crosnier-Lopez M.P., Berre F. Le; Emery J., Suard E., Fourquet J.-L.; 2005; Room temperature crystal structure of $La_{1/3}Zr_2(PO_4)_3$, a NASICON-type compound; Chem. Mater. 17; 6605-6610.

Bohre A., Shrivastava O.P.; 2013; Diffusion of Lanthanum into single-phase sodium zirconium phosphate matrix for nuclear waste immobilization; Radiochemistry 55; 442-449.

Brownfield M.E., Foord E.E., Sutlex S.J., Botinelly T.; 1993;Kosnarite, $KZr_2(PO_4)_3$, a new mineral from Mount Mica and Black Mountain, Oxford County, Maine; Am.Mineral. 78; 653-656.

Bykov D.M., Gobechiya E.R., Kabalov Yu.K., Orlova A.I., Tomilin S.V.; 2006; Crystal structures of lanthanide and zirconium phosphates with general formula $Ln_{0.33}Zr_2(PO_4)_3$, where *Ln*=Ce, Eu, Yb; J. Solid State Chem. 179; 3101-3106.

Bykov D.M., Orlova A.I., Tomilin S.V., Lizin A.A., Lukinykh A.N.; 2005; Americium and plutonium in trigonal phosphates (NZP type) $Am_{1/3}[Zr_2(PO_4)_3]$; Radiochemistry 48, no. 3; 234-239.

Clarke D.R.; 1983; Ceramic material for the immobilization of nuclear waste; Ann. Rev. Mater. Sci. 13; 191-218.

Gobechiya E.R., Kabalov Yu.K., Petkov V.I., Sukhanov M.V.; 2004;Crystal structures of double cesium zirconium and barium zirconium orthophosphates; Crystallogr. Rep. 49, no. 5; 741-746.

Gregg D.J., Karatchevtseva I., Thorogood G.J., Davis J., Bell B.D.C., Jackson M., Dayal P., Ionescu M., Triani G., Short K., Lumpkin G.R., Vance E.R.; 2014; Ion beam irradiation effects in strontium zirconium phosphate with NZP-structure type; J. Nucl. Mater. 446; 224-231.

Hagman L-O., Kierkegaard P.; 1968;The crystal structure of $NaMe_2^{IV}(PO_4)_3$; Me^{IV}=Ge, Ti, Zr; Acta Chem. Scand. 22, no. 4; 1822-1832.

Hazen R.M., Finger L.W., Agrawal D.K., McKinstry H.A., Perrotta A.J.; 1987; High-temperature crystal chemistry of sodium zirconium phostphate (NZP); J. Mater. Res. 2, no. 3; 329-337.

IAEA; 2008; Spent fuel reprocessing options.

IAEA; 2012; http://www.iaea.org/Publications/Factsheets/English/manradwa.html

Law J.D., Garn T.G., Herbst R.S., Meikrantz D.H., Peterman D.R.; 2006; Development of cesium and strontium separation and immobilization technologies in support of an advanced nuclear fuel cycle; WM'06 Conference, February 26 – March 2, Tucson, AZ.

Mingfen W., Bo Yu., Min L., Jing C.; 2012; Coorperation solidification of cesium and strontium; AMR 482-484; 58-61.

Miyajima Y., Saito Y, Matsuoka M., Yamamonoto Y.;1996; Ion conductivity of Nasicon-type $Na_{1+x}M_xZr_{2-x}P_3O_4$; Solid State Ionics 84; 61-64.

Montel J.-M.; 2011; Minerals and design of new waste forms for conditioning nuclear waste; C.R. Geoscience 343; 230-236.

Naik A.H., Deb S.B., Chalke A.B., Saxena M.K., Ramakumar K.L., Venugopal V., Dharwadkar S.R.; 2010; Microwave-assisted low temperature synthesis of sodium zirconium phosphate (NZP) and the leachability of some selected fission products incorporated in its structure – A case study of leachability of cesium; J. Chem. Sci. 122, no. 1; 71-82.

Orlova A.I.; 2002; Isomorphism in crystalline phosphates of the $NaZr_2(PO_4)_3$ structural type and radiochemical problems; Radiochemistry 44, no. 5; 423-445.

Pet'kov V.I., Asabina E.A.; 2004; Thermophysical properties of NZP ceramics (A review); Glass and Ceramics 61; 233-239.

Pet'kov V.I., Asabina E.A.; 2013; Thermodynamic properties of compounds with kosnarite-type structure; Indian J. Chem. 52A; 350-356.

Pet'kov V.I., Kurazhkovskaya V.S., Orlova A.I., Spiridonova M.L.; 2002; Synthesis and crystal chemistry characteristics of the structure of $M_{0.5}Zr_2(PO_4)_3$ phosphates; Crystallogr. Rep. 47, no. 5; 736-743.

Pet'kov V.I., Orlova A.I., Egorkova O.V.; 1996; On the existence of phases with a structure of $NaZr_2(PO_4)_3$ in series of binary orthophosphates with a different alkaline element to zirconium rations; J. Struct. Chem. 37, no. 6; 933-940.

Pet'kov V.I., Shchelokov A.I., Asabina E.A., Kurazhkovskaya V.S., Rusakov D.A., Pokholok K.V., Lazoryak B.I.; 2006; Synthesis and phase formation in $M^{2+}_{0.5(1+x)}Fe_xTi_{2-x}(PO_4)_3$ phosphate series; Russian Journal of Inorganic chemistry 51 no. 12; 1855-1863.

Sims D.J., Andrews W.S., Creber K.A.M.; 2008; Diffusion coefficients for uranium, cesium and strontium in unsaturated prairie soil; J. Radioanal. Nucl. Chem. 277 (1); 143-147.

Somiya A., Roy R.; 2000; Hydrothermal synthesis of fine oxide powders; Bull. Mater. Sci. 23 (3); 453-460.

Sugantha M., Kumar N.R.S., Varadaraju U.V.; 1998; Synthesis and leachability studies of NZP and eulytine phases; Waste Manage. 18; 275-279.

Sugantha M., Varadaraju U.V.; 1994; Synthesis and characterization of NZP phases, $AM^{'3+}M^{''4+}P_3O_{12}$; J. Solid State Chem. 111; 33-40.

Todd T.A., Batcheller T.A., Law J.D., Herbst R.S.; 2004; Cesium and strontium separation technologies literature review; Idaho National Engineering and Environmental Laboratory.

Todd T.A., Law J.D., Herbst R.S., Meikrantz D.H., Peterman D.R., Riddle C.L., Tillotson R.D.; 2005; Advanced technologies for the simultaneous separation of cesium and stronitum from spent nuclear fuel; WM'05 Conference, February 27 - March 3, Tucson, AZ.

Vance E.R., 2012; “Ceramic waste forms” in Konings R.J.M (ed.) Comprehensive nuclear materials, volume 5.

Verhoef E., Neeft E., Grupa J., Poley A.; 2011; Outline of a disposal concept in clay; COVRA N.V.

Warin D.M.; 2011; Developments in the partitioning and transmutation of radioactive waste; CEA/Marcoule, France; 363-376.

West A.R.; 1984; Solid state chemistry and its applications; John Wiley & Sons Ltd.

Xu C., Wang J., Chen J.; 2012; Solvent extraction of strontium and cesium: a review of recent progress; Solvent Extr. Ion Exch. 30; 623-650.